Journal Pre-proofs

Stochastic Measurement of Wind Power Using a Two-Bit A/D Converter

Vladimir Vujicic, Boris Licina, Dragan Pejic, Platon Sovilj, Aleksandar Radonjic

PII: S0263-2241(19)31050-4
DOI: https://doi.org/10.1016/j.measurement.2019.107184
Reference: MEASUR 107184

To appear in: *Measurement*

Received Date: 25 March 2019
Revised Date: 5 August 2019
Accepted Date: 19 October 2019

Please cite this article as: V. Vujicic, B. Licina, D. Pejic, P. Sovilj, A. Radonjic, Stochastic Measurement of Wind Power Using a Two-Bit A/D Converter, *Measurement* (2019), doi: https://doi.org/10.1016/j.measurement.2019.107184

Stochastic Measurement of Wind Power Using a Two-Bit A/D Converter

Vladimir Vujicic, Boris Licina, Dragan Pejic, Platon Sovilj and Aleksandar Radonjic

1. Vladimir Vujicic, Institute of Technical Sciences of the Serbian Academy of Sciences and Arts, 11000 Belgrade, Serbia 2. Boris Licina, Faculty of Technical Sciences, University of Novi Sad,

21000 Novi

Sad, Serbia,

3. Dragan Pejic (corresponding author), Faculty of Technical Sciences, University of Novi Sad, 21000 Novi Sad, Serbia (email: pejicdra@uns.ac.rs), 4. Platon Sovilj, Faculty of Technical Sciences, University of Novi Sad,

21000 Novi

Sad, Serbia,

5. Aleksandar Radonjic, Institute of Technical Sciences of the Serbian Academy of Sciences and Arts, 11000 Belgrade, Serbia

***Abstract*: This paper presents a new method for stochastic measurement of wind power and energy. Compared to the existing approaches, this method has two advantages: first, it is much simpler and cheaper to implement, and second, it can be easily integrated with cup anemometers. In this way, it is possible to construct a low-cost mobile device capable of measuring wind power and energy. In order to prove the validity of our method, we have conducted several laboratory experiments. The obtained results have shown that, over the time interval of 100 seconds, wind power and energy can be measured with an accuracy of 0.09 %.**

***Keywords*: Stochastic measurements, two-bit A/D conversion, anemometer with cups, wind power, wind energy.**

1. Introduction

With gradual exhaustion of fossil fuels, researchers are increasingly focusing on new energy sources. Among them, the wind power is particularly valued due to its clean pollution and wide distribution of resources. However, the main problem of using wind as a source of power is unstable output power. The stochastic and unpredictable nature of wind may cause significant fluctuations in voltage and frequency, and thus, interference and problems with the grid. So,

before constructing a wind farm, it is necessary to perform measurements of wind speed. Based on them, it is possible to calculate wind power and its variation over time.

Unfortunately, today there is no cheap way to measure wind power and energy. Most measurements are done using expensive instruments such as SODAR and LIDAR [1], [2]. Apart from being expensive, these instruments are not easy to transport, which further complicates their use. On the other hand, there are numerous devices for measuring wind speed, such as anemometers with cups [3] and ultrasonic anemometers [4]. These devices generate signals (analog [3] or digital [4]) whose amplitudes are proportional to the wind speed, and hence, they can be used as a basis for designing wind power (energy) meters. This possibility arises from the fact that wind power (energy) is cubically related to wind speed [1].

Table 1. Notations used in this paper.

Symbol	Meaning
$f_i(t)$	Input signal in the i-th channel
Ψ_i	Result of A/D conversion in the i-th channel
$2g$	Quantum of a two-bit A/D converter
T	Measurement interval
N	Number of samples in the measurement interval T

Having this in mind, in this paper, we present a simple and cheap approach to measure wind power and energy. The key idea behind this approach is to use stochastic digital measurement method (SDMM) [5]-[13] to process the data generated by anemometer with cups. Unlike the standard sampling method [14], the SDMM can be realized using two-bit A/D converters. Hence, its integration with an anemometer represents a natural step towards designing a low-cost mobile device capable of measuring wind power and energy.

The organization of this paper is as follows: Section 2 deals with the background of stochastic measurement of wind power and energy. Theoretical analysis and experimental results are given in Section 3, while Section 4 concludes the paper. For ease of reading, a list of notations is given in Table 1.

II. Stochastic Measurement of Wind Power

A. Wind Speed and Wind Power

From physics it is known that the kinetic energy of an object depends on its speed and mass. In other words, it is calculated as $(1/2)\cdot m\cdot v^2$, where v is speed and m is the mass. In the case of wind, m is obtained from the product of air density ρ and its volume. As the air is constantly in motion, the volume is calculated by multiplying the wind's speed by the area A through which it passes during a time period t. This leads to the equations

$$P_w = \frac{1}{2} \cdot A \cdot \rho \cdot v^3 \quad (1)$$

$$E_w = \bar{P}_w \cdot t = \frac{1}{2} \cdot A \cdot \rho \cdot \overline{v^3} \cdot t \quad (2)$$

where P_w and E_w denote wind power and energy, respectively. Unfortunately, the electrical power and energy, extracted from wind generators, are quite lower than those given by (1)-(2). More precisely, they are equal to

$$P_e = C_p \cdot P_w = \frac{1}{2} \cdot A \cdot \rho \cdot C_p \cdot v^3 \quad (3)$$

$$E_e = C_p \cdot E_w = \frac{1}{2} \cdot A \cdot \rho \cdot C_p \cdot \overline{v^3} \cdot t \quad (4)$$

where C_p denotes the power coefficient of a wind turbine. Its maximum value is equal to 0.593, and it is called the Betz limit [1]. In practice, however, the value of the C_p is substantially lower and varies between 0.35 and 0.45.

B. Generalization of a Two-bit SDMM

As already stated, the SDMM can be realized using two-bit A/D converters. Such an approach is possible only if we add a dither noise to the input signal before its digitalization. For instance, if we want to measure the mean value of the signal $f_1(t)$ we need to add a dither noise h_1 (Fig. 1). In that case, the output value $\bar{\Psi}$ will be equal to [12]

$$\bar{\Psi}(1) = \frac{1}{N} \cdot \sum_{i=1}^{N} \Psi_1(i) = \frac{1}{T} \cdot \int_0^T f_1(t)\, dt \quad (5)$$

On the other hand, since the error is defined by $e = \Psi(1) - f_1(t)$, the variance of the average error will be equal to

$$\sigma_e^2(1) = \frac{1}{N} \cdot \left[\frac{2g}{T} \cdot \int_0^T \left| f_1(t) \right| dt - \frac{1}{T} \cdot \int_0^T f_1^2(t)\, dt \right]. \tag{6}$$

Similarly, if one wants to measure a product of two signals $f_1(t)$ and $f_2(t)$ it is necessary to add two uncorrelated dithers h_1 and h_2 (Fig. 2). In that case, it will hold that [5]

$$\bar{\Psi}(2) = \frac{1}{N} \cdot \sum_{i=1}^{N} \Psi_1(i) \cdot \Psi_2(i) = \frac{1}{T} \cdot \int_0^T f_1(t) \cdot f_2(t)\, dt \tag{7}$$

On the contrary to the previous scenario, in this one, the error is defined by $e = \Psi(2) - f_1(t) \cdot f_2(t)$. As a result, the average error variance will be equal to

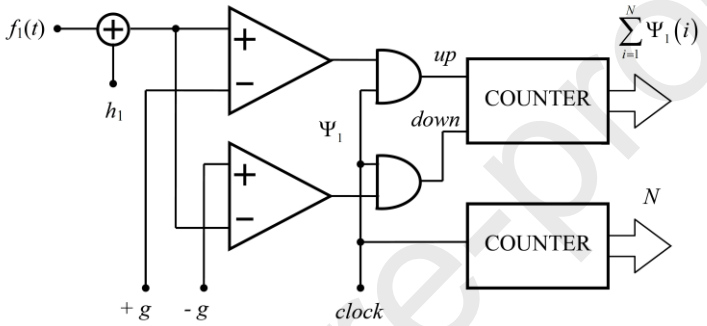

Fig. 1. Block diagram of the device for measuring the mean value of the input signal.

$$\sigma_e^2(2) = \frac{1}{N} \cdot \left[\frac{(2g)^2}{T} \cdot \int_0^T \left| f_1(t) \cdot f_2(t) \right| dt - \frac{1}{T} \cdot \int_0^T f_1^2(t) \cdot f_2^2(t)\, dt \right] \tag{8}$$

In general, it can be shown (Appendix A) that the expressions

$$\bar{\Psi}(k) = \frac{1}{N} \cdot \sum_{i=1}^{N} \Psi_1(i) \cdot \Psi_2(i) \cdots \Psi_k(i) = \frac{1}{T} \cdot \int_0^T f_1(t) \cdot f_2(t) \cdots f_k(t)\, dt$$

(9)

$$\sigma_e^2(k) = \frac{1}{N} \cdot \left[\frac{(2g)^k}{T} \cdot \int_0^T \left| f_1(t) \cdot f_2(t) \cdots f_k(t) \right| dt - \frac{1}{T} \cdot \int_0^T f_1^2(t) \cdot f_2^2(t) \cdots f_k^2(t)\, dt \right] \tag{10}$$

are valid for any $k \geq 1$. From this, it is easy to see that a two-bit SDMM can be used to measure a product of k input signals. In this paper, we will restrict ourselves to the case when $k = 3$.

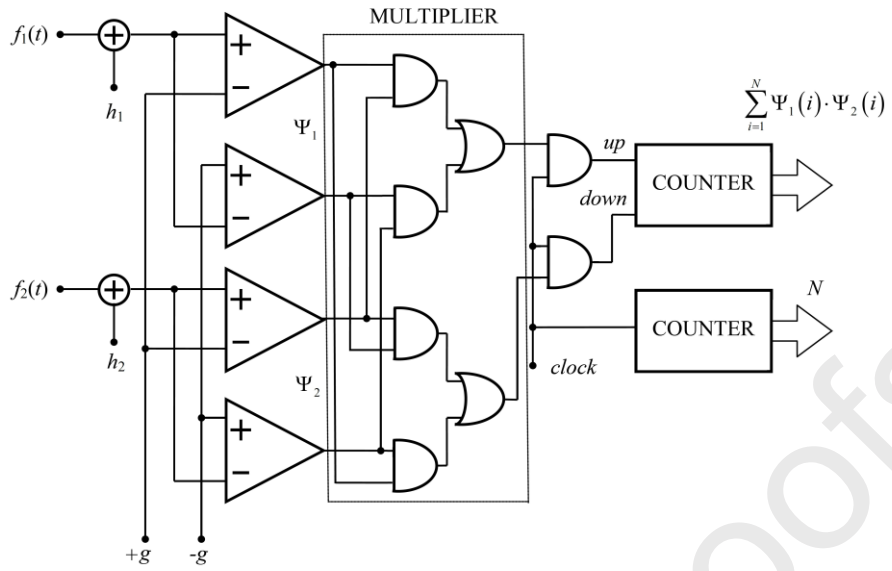

Fig. 2. Block diagram of the device for measuring a product of two input signals.

C. Instrument Scheme

In the Section II-A it is shown that the wind power (energy) is cubically related to the speed of the wind. In the context of the aforementioned, one might think that the scheme from Fig. 3. is suitable for measuring wind power and energy. The only condition, in this regard, is that the signals h_1, h_2 and h_3 are mutually uncorrelated (Fig. 3).

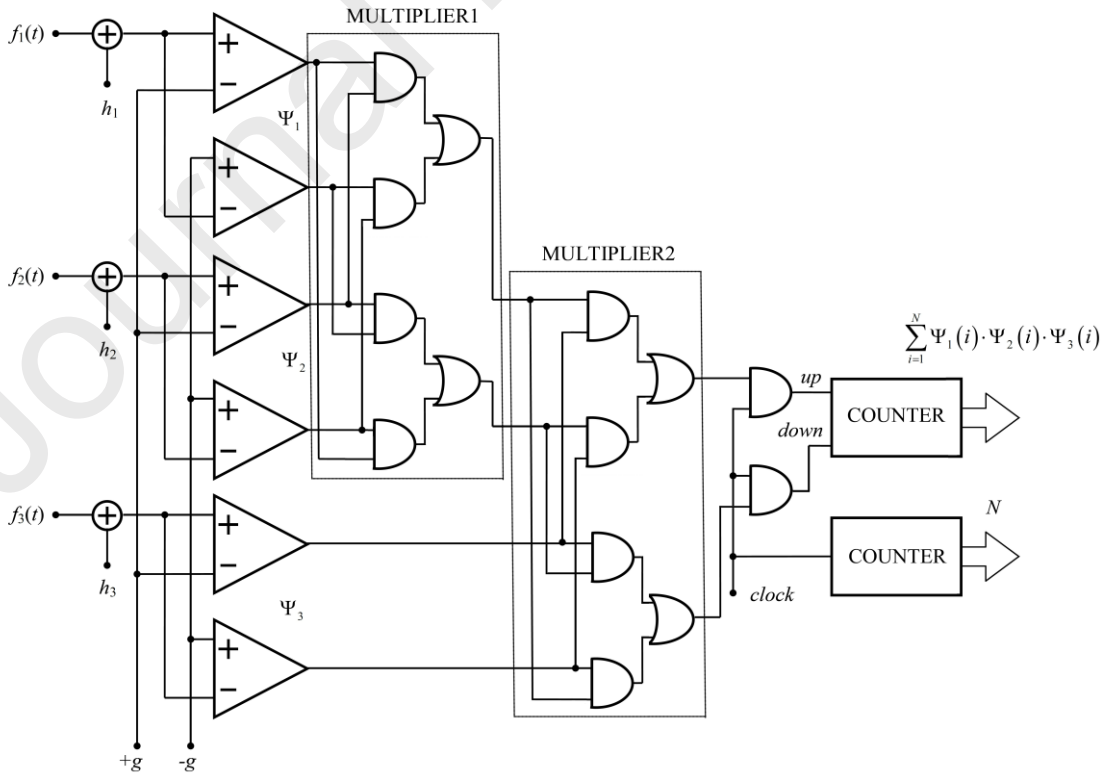

Fig. 3. Block diagram of the device for measuring a product of three input signals.

However, in this particular case, the above scheme is not applicable. The reason is that an anemometer with cups generates a sinusoid whose amplitude and frequency are proportional to the wind speed. Hence, by applying the above scheme, the output value would be equal to zero (the mean value of a sinusoid raised to an odd power greater than 2 is equal to zero). To avoid such scenario we will measure the absolute value of a sinusoid raised to the third power. For that purpose, it can be used the scheme shown in Fig. 4.

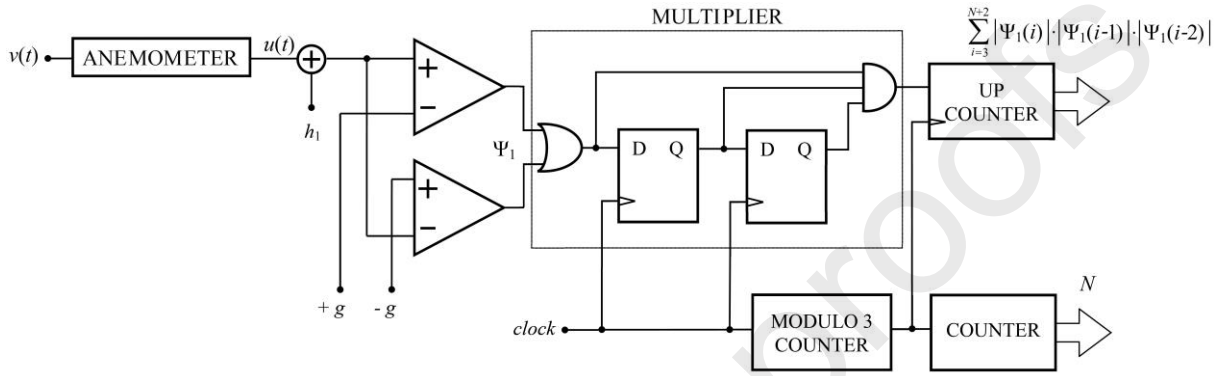

Fig. 4. Block diagram of the device for measuring the absolute value of the input signal raised to the third power.

The first thing we notice from the above scheme is that is that there is only one input channel. Such solution is possible due to very low frequency of the input signal $u(t)$. Namely, if the input signal has a low frequency and if it is digitized using a fast A/D converter, several adjacent samples of $u(t)$ will have an identical or nearly identical values (depending on the sampling rate). In our case, the multiplication of three adjacent samples (within one group) is equivalent to the digitization of a sinusoid raised to the third power. If this process is performed using a two-bit A/D converter, the output samples will have three values: 10 ("+1"), 00 ("0") and 01 ("-1") (the output 11 is forbidden) [9]. From this, it is easy to conclude that the two-input OR gate has the role to convert "negative" samples into the "positive" ones (Fig. 4). Also, we see that the up-counter will increase its value only if three adjacent bits have the value 1. Finally, the role of modulo-3 counter is to ensure that the the output samples (bits) are processed in groups of three.

III. Theoretical Analysis and Experimental Verification

A. Theoretical Analysis

To make the theoretical analysis comparable with experimental results, we need to consider the systematic errors (voltage offsets) caused by the imperfections of the measuring device (Fig. 4). They can be grouped into two different categories: the errors caused by comparators' offsets

and the error induced by the analog adder. In [11] it was shown that using the cross-switching method the first group of errors can be suppressed by more than 80 dB. Hence, they become negligible. However, as the method from [11] cannot suppress (eliminate) the error induced by the analog adder (Fig. 5), it is necessary to analyze its impact on the measurement result.

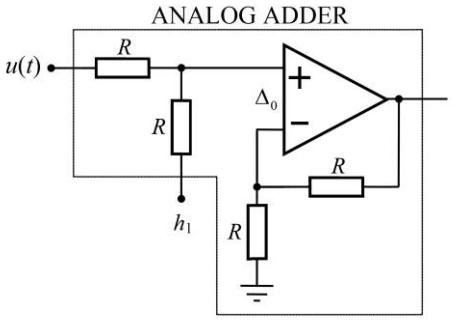

Fig. 5. Structure of the analog adder.

Accordingly, let us suppose that Δ_0 denotes the voltage offset of the analog adder and that the input signal has the form $u(t) = U \cdot sin(\omega t)$, where 0.5 V ≤ U ≤ 4.5 V. In that case, the output value $\overline{|u|^3}$ will be equal to

$$\overline{|u|^3} = \frac{1}{N} \cdot \sum_{i=1}^{N} \left|\Psi_1(i)\right|^3 = \frac{1}{T} \int_0^T \left|\Delta_0 + U \cdot sin(\omega t)\right|^3 dt \tag{11}$$

i.e.

$$\overline{|u|^3} = \frac{1}{T} \int_0^T \left|{\Delta_0}^3 + 3\Delta_0^2 \cdot U \cdot sin(\omega t) + 3\Delta_0 \cdot U^2 \cdot sin^2(\omega t) + U^3 \cdot sin^3(\omega t)\right| dt \tag{12}$$

Considering that $|\Delta_0|$ is in the range of a few mV [15], the above equality reduces to

$$\overline{|u|^3} \approx \frac{1}{T} \int_0^T U^2 \cdot sin^2(\omega t) \cdot \left|3\Delta_0 + U \cdot sin(\omega t)\right| dt \tag{13}$$

Now, if $\Delta_0 > 0$, it will hold that

$$\overline{|u|^3} \approx \frac{1}{T} \int_0^{T/2} U^2 \cdot sin^2(\omega t) \cdot [3\Delta_0 + U \cdot sin(\omega t)]\, dt + \frac{1}{T} \int_{T/2}^{T} U^2 \cdot sin^2(\omega t) \cdot [-3\Delta_0 - U \cdot sin(\omega t)]\, dt \tag{14}$$

i.e.

$$\overline{|u|^3} \approx \frac{2}{T} \int_0^{T/2} U^3 \cdot sin^3(\omega t)\, dt = \frac{4}{3\pi} \cdot U^3 \tag{15}$$

It is easy to show that the same result holds for $\Delta_0 < 0$. In other words, Δ_0 has the same value in both half-periods, but an opposite sign. Hence, it can be concluded that the voltage offset of the analog adder has no impact on the measurement result. Bearing this in mind, let us determine the variance of the average error e. According to (10), it has the form

$$\sigma_{\bar{e}}^2(3) = \frac{1}{N} \cdot \left[\frac{(2g)^3}{T} \cdot \int_0^T \left| U \cdot \sin(\omega t) \right|^3 dt - \frac{1}{T} \int_0^T \left| U \cdot \sin(\omega t) \right|^6 dt \right] \tag{16}$$

i.e.

$$\sigma_{\bar{e}}^2(3) = \frac{1}{N} \cdot \left[\frac{(2g)^3}{T} \cdot \int_0^T \left| U \cdot \sin(\omega t) \right|^3 dt - \frac{1}{T} \int_0^T \left| U \cdot \sin(\omega t) \right|^6 dt \right] \tag{17}$$

To calculate the above integrals, we can use the equalities [16]

$$\int \sin^3 x \cdot dx = \frac{\cos^3 x}{3} - \cos x$$

$$\int \sin^6 x \cdot dx = \frac{x}{16} - \frac{3}{16} \cdot \sin 2x - \frac{1}{16} \cdot \left(\sin 2x - \frac{\sin^3 2x}{3} \right) + \frac{3}{16} \cdot \left(x + \frac{\sin 4x}{4} \right)$$

Based on them, it is easy to show that

$$\sigma_{\bar{e}}^2(3) = \frac{U^3}{3\pi N} \cdot \left(32 \cdot g^3 - \frac{30\pi + 4}{32\pi} \cdot U^3 \right) \tag{18}$$

B. Laboratory Experiments

To validate the above theory, we have conducted several laboratory experiments. For that purpose, two instruments were used: the prototype instrument for measuring the RMS value (PIM-RMS) of the sine voltage (Fig. 6a) and the phase angle standard (PAS) (Fig. 6b) [17].

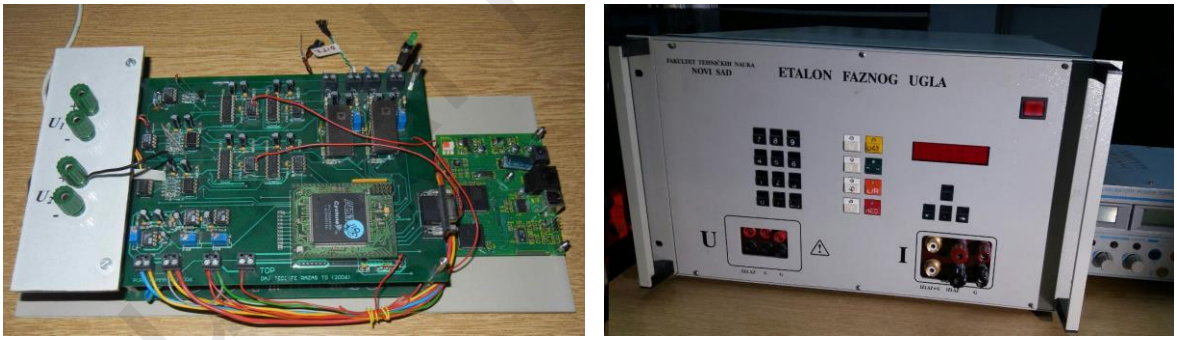

(a) (b)

Fig. 6. Photos of the instruments used in laboratory experiments:
(a) the PIM-RMS and (b) the PAS.

The first instrument operates at a sampling frequency of 0.1 MHz and digitizes the input signal into a two-bit output stream. For that purpose, it also uses the method for suppressing the errors caused by comparators' offsets [11]. In this way, it is possible to measure the mean value of the square of the sine voltage with accuracy better than $\gamma = 80$ ppm [8].

The second instrument has several functional blocks including two-channel digital function generator. In our experiments, this block was used as a signal generator. Its main characteristics are as follows:

1) frequency range 10 Hz–10 kHz,

2) voltage range 0–120 V,

3) current range 0–6 A,

4) output power: voltage channel 25 W, current channel 100 W,

6) phase angle: 0º–360º,

7) phase angle resolution: equivalent to time delay of 5 ns in high-speed operation,

8) stability of signal generation: a few ppm of full scale per year,

9) accuracy of signal generation: 12 ppm of full scale.

The experiments were started by generating sine wave voltages with frequencies 10 Hz and 20 Hz amplitudes up to 4.5 V. The PAS was connected at the input of the PIM-RMS, whereas the PIM-RMS was connected to the PC via RS-232 serial link. The sampling frequency was set to 25 kHz and each experiment lasted 100 seconds. The groups of three adjacent samples were treated as individual samples, meaning that $25 \cdot 10^3 \cdot 100/3 = 833333$ samples per one experiment was processed. The obtained results are shown in Table 2.

Table 2. Results of the laboratory experiments.

	1	2	3	4	5	6	7	8	9
	U	f	$\overline{\lvert u\rvert_{ex}^3}$	$\overline{\lvert u\rvert_m^3}$	$\delta \cdot \overline{\lvert u\rvert_{\max}^3}$	$\sigma_{\bar{e}}$	$2 \cdot \sigma_{\bar{e}} + \delta \cdot \overline{\lvert u\rvert_{\max}^3}$	$\left\lvert \overline{\lvert u\rvert_m^3} - \overline{\lvert u\rvert_{ex}^3} \right\rvert$	$\dfrac{\left\lvert \overline{\lvert u\rvert_m^3} - \overline{\lvert u\rvert_{ex}^3} \right\rvert}{\overline{\lvert u\rvert_{\max}^3}}$
	V	Hz	V^3	V^3	V^3	V^3	V^3	V^3	%
1	4.500	20	38.675	38.702	0.00637	0.0505	0.1074	0.027	0.05
2	4.000	10	27.162	27.150	0.00637	0.0497	0.1057	0.012	0.02
3	3.500	20	18.197	18.156	0.00637	0.0448	0.0960	0.041	0.08
4	3.000	10	11.459	11.482	0.00637	0.0379	0.0822	0.023	0.04
5	2.500	20	6.631	6.636	0.00637	0.0300	0.0664	0.005	0.01
6	2.000	10	3.395	3.444	0.00637	0.0220	0.0504	0.049	0.09
7	1.500	20	1.432	1.439	0.00637	0.0145	0.0354	0.007	0.01
8	1.000	10	0.424	0.403	0.00637	0.0079	0.0222	0.021	0.04
9	0.500	20	0.053	0.064	0.00637	0.0028	0.0120	0.011	0.02

The first two columns show the parameters of the signals generated by the PAS. Exact and measured values of $\overline{|u|^3}$ are displayed in the third and fourth columns, respectively. The fifth column shows the results of the estimated absolute error of measuring $\overline{|u|^3}$ using the PIM-RMS.

It can be observed that this error is completely deterministic (Appendix B). Unlike it, the variance of the average error is stochastic and depends on the waveform of the input signal (sixth column). The seventh and eight columns, respectively, show the expectable uncertainty of measurement (with a coverage factor of $k = 2$) and the absolute difference between mesured and exact results. Finally, the ninth column shows the relative measurement uncertainty. From it, it can be seen that the PIM-RMS measures the absolute value of the input signal raised to the third

power with accuracy of 0.09 %. The same results applies to the measurement of wind power and energy, since the parameters A, ρ and t are known with much higher accuracy (Appendix C).

5. Conclusion

Accurate measurement of wind power (energy) is a necessary condition for the development of new types of wind power generators. In this paper, it is shown that intergrating a two-bit SDMM with cup anemometers yields a simple solution for measuring of wind power and energy. The presented method is theoretically analyzed and empirically verified through several experiments. The obtained results demonstrate that**,** over the time interval of 100 seconds, wind power (energy) can be measured with an accuracy of 0.09 %. Thanks to this feature, the proposed method represents a solid basis for the design of high-precision instruments as a low-cost alternative to those based on standard sampling method.

References

[1] P. Jain, *Wind Energy Engineering*, 2nd ed., The McGraw Hill Companics, Inc., 2016.

[2] J. F. Manwell, J. G. McGowan, A. L. Rogers, *Wind Energy Explained: Theory, Design and Application*, 2nd ed., John Wiley & Sons Ltd., 2010.

[3] M. Zlatanovic and V. Zlatanovic, "Long Term Operation Characteristics of NRG #40 Cup Anemometers," in *Proceedings of the EWEA Annual Event*, pp. 1–10, EWEA, Apr. 2012.

[4] L. Pugi *et al.*, "Integrated Design and Testing of an Anemometer for Autonomous Sail Drones,", *J. Dyn. Sys. Meas. Control*, vol. 140, no. 5, pp. 1–10, May. 2018.

[5] V. Vujicic *et al.*, "Low Frequency Stochastic True RMS Instrument," *IEEE Trans. Instrum. Meas.*, vol. 48, no. 2, pp. 467-470, Apr. 1999.

[6] D. Pejic and V.Vujicic, "Accuracy Limit of High-Precision Stochastic Watthour Meter," *IEEE Trans. Instrum. Meas.*, vol. 49, no. 3, pp. 617-620, Jun. 2000.

[7] V. Vujicic, "Generalized Low-Frequency Stochastic True RMS Instrument," *IEEE Trans. Instrum. Meas.*, vol. 50, no. 5, pp. 1089-1092, Oct. 2001.

[8] D. Pejic, "Stochastic Measurement of Electric Power and Energy (in Serbian)," PhD thesis, Faculty of Technical Sciences, University of Novi Sad, 2010.

[9] A. Radonjic, P. Sovilj and V. Vujicic, "Stochastic Measurement of Power Grid Frequency Using a Two-Bit A/D Converter," *IEEE Trans. Instrum. Meas.*, vol. 63, no. 1, pp. 56-62, Jan. 2014.

[10] Z. Beljic *et al.*, "Grid Fundamental Harmonic Measurement in Presence of Gaussian Frequency Deviation using 2-bit Flash A/D Converter", *Technical Gazette*, vol. 24, no. 2, pp. 481-488, Apr. 2017.

[11] M. Urekar *et al.*, "Accuracy Improvement of the Stochastic Digital Electrical Energy Meter," *Measurement*, vol. 98, pp. 139-150, Feb. 2017.

[12] B. Vujicic, "Null Detection Using a Low Resolution A/D Converter (in Serbian)," PhD thesis, Faculty of Technical Sciences, University of Novi Sad, 2017.

[13] D. Pejic *et al.*, "Stochastic Digital DFT Processor and Its Application to Measurement of Reactive Power and Energy," *Measurement*, vol. 124, pp. 494–504, Aug. 2018.

[14] G. D'Antona and A. Ferrero, Digital Signal Processing for Measurement Systems: Theory & Applications, Springer Science Inc., 2006.

[15] A. Kay, *Operational Amplifier Noise: Techniques and Tips for Analyzing and Reducing Noise*, Elsevier Inc., 2012.

[16] R. Larson and B. Edwards, *Calculus of a Single Variable: Early Transcendental Functions*, 6th ed., Cengage Learning, 2015.
[17] Z. Mitrovic, "A Phase Angle Standard," *Meas. Sci. Technol.*, vol. 15, no. 3, pp. 559-564, Mar. 2004.

APPENDIX A

Suppose that, over the time interval T, the product of k signals is measured with a two-bit SDMM. In that case, the output value $\bar{\Psi}$ of the multiplier consisting of $k-1$ binary multipliers will be equal to

$$\bar{\Psi}(k) = \frac{1}{N} \cdot \sum_{i=1}^{N} \Psi_1(i) \cdot \Psi_2(i) \cdots \Psi_k(i) = \frac{1}{T} \cdot \int_0^T f_1(t) \cdot f_2(t) \cdots f_k(t)\, dt \tag{A1}$$

where $\Psi_1(i)$, $\Psi_2(i)$,...,$\Psi_k(i)$ are the digitized values of k input signals and where $N \to \infty$ denotes the unlimited number of samples (caused by unlimited sampling frequency) within T. Now, we can state the following theorem.

Theorem 1. *Let* $\sigma_{\bar{e}}^2(k) = \dfrac{\sigma_e^2(k)}{N}$ *be the variance of the average error for product of k signals measured with a two-bit SDMM over the interval [0, T]. Then, for finite value of N*

$$\sigma_{\bar{e}}^2(k) = \frac{1}{N} \cdot \left[\frac{(2g)^k}{T} \cdot \int_0^T \left| f_1(t) \cdot f_2(t) \cdots f_k(t) \right| dt - \frac{1}{T} \cdot \int_0^T f_1^2(t) \cdot f_2^2(t) \cdots f_k^2(t)\, dt \right] \tag{A2}$$

Proof. Instead of strict and long proof by mathematical induction, we give a simple analysis (in the spirit of mathematical induction) that confirms the general formula.

Step 1. For $k = 1$, the output value is equal to

$$\psi = f_1(t) + e \tag{A3}$$

and the variance of the average error is given by

$$\sigma_e^2(1) = \frac{1}{N} \cdot \left[\frac{2g}{T} \cdot \int_0^T \left| f_1(t) \right| dt - \frac{1}{T} \cdot \int_0^T f_1^2(t)\, dt \right] \tag{A4}$$

Step 2. For $k = 2$, the output value is equal to

$$\psi = f_1(t) \cdot f_2(t) + e \tag{A5}$$

and the variance of the average error is given by

$$\sigma_{\bar{e}}^2(2) = \frac{1}{N} \cdot \left[\frac{(2g)^2}{T} \cdot \int_0^T \left| f_1(t) \cdot f_2(t) \right| dt - \frac{1}{T} \cdot \int_0^T f_1^2(t) \cdot f_2^2(t)\, dt \right] \tag{A6}$$

Step 3. Observe that the expressions (A4) and (A6) can be written as

$$\sigma_{\bar{e}}^2(1) = \frac{1}{N} \cdot \left[\frac{(2g)^0 \cdot 2g}{T} \cdot \int_0^T |1| \cdot \left| f_1(t) \right| dt - \frac{1}{T} \cdot \int_0^T [1^2 \cdot f_1^2(t)]\, dt \right] \tag{A7}$$

$$\sigma_e^2(2) = \frac{1}{N} \cdot \left[\frac{(2g)^1 \cdot 2g}{T} \cdot \int_0^T \left| f_1(t) \right| \cdot \left| f_2(t) \right| dt - \frac{1}{T} \cdot \int_0^T [\, f_1^2(t) \cdot f_2^2(t)\,]\, dt \right] \tag{A8}$$

In addition, observe that for any $k \geq 1$ when adding the next function and the next multiplier:

a) the first integral is multiplied with $2g$,

b) the function within the first integral is multiplied with the absolute value of the next function,

c) the function within the second integral is multiplied with the square of the next function,

Step 4. Suppose that the theorem is true for some k and also a), b) and c). It remains to show that it holds for $k + 1$.

$$\sigma_e^2(k+1) = \frac{1}{N} \cdot \left[\frac{(2g)^k \cdot 2g}{T} \cdot \int_0^T \left| f_1(t) \cdot f_2(t) \cdots f_k(t) \right| \cdot \left| f_{k+1}(t) \right| dt - \frac{1}{T} \cdot \int_0^T [f_1^2(t) \cdot f_2^2(t) \cdots f_k^2(t)] \cdot f_{k+1}^2(t)\, dt \right] \tag{A9}$$

When the indicated operations are performed, we obtain

$$\sigma_e^2(k+1) = \frac{1}{N} \cdot \left[\frac{(2g)^{k+1}}{T} \cdot \int_0^T \left| f_1(t) \cdot f_2(t) \cdots f_{k+1}(t) \right| dt - \frac{1}{T} \cdot \int_0^T f_1^2(t) \cdot f_2^2(t) \cdots f_{k+1}^2(t)\, dt \right] \tag{A10}$$

which proves the theorem.

APPENDIX B

Let γ and ε be the relative measurement errors of $\overline{|u|^2}$ and $\sqrt{\overline{|u|^2}}$, respectively. In that case, we can write

$$\overline{|u|_m^2} = \overline{|u|_{ex}^2} \cdot (1+\gamma) \tag{B1}$$

$$\sqrt{\overline{|u|_m^2}} = \sqrt{\overline{|u|_{ex}^2}} \cdot (1+\varepsilon) \tag{B2}$$

where $\overline{|u|_{ex}^2}$ and $\sqrt{\overline{|u|_{ex}^2}}$ denote the exact values of $\overline{|u|^2}$ and $\sqrt{\overline{|u|^2}}$, respectively. With this in mind, suppose that $\varepsilon << 1$ (this assumption is very reasonable in practice). In that case, the expression (B2) can be written as

$$\overline{|u|_m^2} = \overline{|u|_{ex}^2} \cdot (1+\varepsilon)^2 = \overline{|u|_{ex}^2} \cdot (1+2\varepsilon+\varepsilon^2) \approx \overline{|u|_{ex}^2} \cdot (1+2\varepsilon) \tag{B3}$$

wherefrom it follows that

$$\varepsilon = \gamma/2 \tag{B4}$$

In a similar way, let δ and ξ be the relative measurement errors of $\overline{|u|^3}$ and $\sqrt{\overline{|u|^3}}$, respectively. In that case, we can write

$$\overline{|u|_m^3} = \overline{|u|_{ex}^3} \cdot (1+\delta) \tag{B5}$$

$$\sqrt{\overline{|u|_m^3}} = \sqrt{\overline{|u|_{ex}^3}} \cdot (1+\xi) \tag{B6}$$

where $\overline{|u|_{ex}^3}$ and $\sqrt{\overline{|u|_{ex}^3}}$ denote the correct values of $\overline{|u|^3}$ and $\sqrt{\overline{|u|^3}}$, respectively. Now, since $\xi << 1$, the expression (B6) can be written as

$$\overline{|u|_m^3} = \overline{|u|_{ex}^3} \cdot (1+\xi)^3 = \overline{|u|_{ex}^3} \cdot (1+3\xi+3\xi^2+\xi^3) \approx \overline{|u|_{ex}^3} \cdot (1+3\xi) \tag{B7}$$

wherefrom it follows that

$$\xi = \delta/3 \tag{B8}$$

If dithering signals h_1, h_2 and h_3 are mutually uncorrelated, the measurement accuracy of any SDMM-based device will depend only on its deterministic components. Hence, it follows that

$$\varepsilon \approx \xi \tag{B9}$$

i.e.

$$\delta \approx 3\varepsilon \tag{B10}$$

In other words, the estimated accuracy of the PIM-RMS, in the case of measurement of $\overline{|u|^3}$, is not worse that 3·40 ppm = 120 ppm.

APPENDIX C

The total wind energy E_R is calculated as

$$E_R = \frac{1}{2} \cdot A \cdot \rho \cdot \overline{v^3} \cdot t \tag{C.1}$$

Now, let dE_R be the uncertainty of the measurement of total wind energy. In that case, the relative uncertainty of the measurement of total wind energy can be expressed as

$$\frac{dE_R}{E_R} = \frac{dA}{A} + \frac{d\rho}{\rho} + \frac{d\overline{v^3}}{\overline{v^3}} + \frac{dt}{t} \tag{C.2}$$

However, as the relative uncertainties of measurement of multiplicative constants (A, ρ) and time t are extremely small (they are known with a very high accuracy), it follows that

$$\frac{dE_R}{E_R} \approx \frac{d\overline{v^3}}{\overline{v^3}} = \frac{d\overline{|u|^3}}{\overline{|u|^3}} \tag{C.3}$$

- We propose a new method for stochastic measurement of wind power and energy.
- The experimental results show that wind power and energy can be measured with an accuracy of 0.09 %.
- The proposed method can be easily implemented in hardware.
- The proposed method can be easily integrated with cup anemometers.